

# Flight Performance of the AKARI Cryogenic System

Takao NAKAGAWA,<sup>1,2</sup> Keigo ENYA,<sup>1</sup> Masayuki HIRABAYASHI,<sup>3</sup> Hidehiro KANEDA,<sup>1</sup>  
Tsuneo KII,<sup>1</sup> Yoshiyuki KIMURA,<sup>3</sup> Toshio MATSUMOTO,<sup>1</sup> Hiroshi MURAKAMI,<sup>1</sup>  
Masahide MURAKAMI,<sup>4</sup> Katsuhiko NARASAKI,<sup>3</sup> Masanao NARITA,<sup>1</sup> Akira OHNISHI,<sup>1</sup>  
Shoji TSUNEMATSU,<sup>3</sup> and Seiji YOSHIDA<sup>3</sup>

<sup>1</sup>*Institute of Space and Astronautical Science, Japan Aerospace Exploration Agency,  
3-1-1 Yoshinodai, Sagami-hara, Kanagawa 228-0024, Japan*

<sup>2</sup>*nakagawa@ir.isas.jaxa.jp*

<sup>3</sup>*Sumitomo Heavy Industries, Ltd. 5-2 Soubiraki-cho, Niihama, Ehime 791-8588, Japan*

<sup>4</sup>*University of Tsukuba, 1-1-1 Ten-nodai, Tsukuba, Ibaraki 305-8571, Japan*

(Received 2007 May 31; accepted 2007 August 9)

## Abstract

We describe the flight performance of the cryogenic system of the infrared astronomical satellite AKARI, which was successfully launched on 2006 February 21 (UT). AKARI carries a 68.5 cm telescope together with two focal plane instruments, Infrared Cameras (IRC) and Far Infrared Surveyor (FIS), all of which are cooled down to cryogenic temperature to achieve superior sensitivity. The AKARI cryogenic system is a unique hybrid system, which consists of cryogen (liquid helium) and mechanical coolers (2-stage Stirling coolers). With the help of the mechanical coolers, 179 L (26.0 kg) of super-fluid liquid helium can keep the instruments cryogenically cooled for more than 500 days. The on-orbit performance of the AKARI cryogenics is consistent with the design and pre-flight test, and the boil-off gas flow rate is as small as 0.32 mg/s. We observed the increase of the major axis of the AKARI orbit, which can be explained by the thrust due to thermal pressure of vented helium gas.

**Key words:** infrared: general - instrumentation: miscellaneous - space vehicles: instruments

## 1. Introduction

In order to achieve superior sensitivity, infrared telescopes in space must be cooled down to cryogenic temperatures. IRAS (Neugebauer et al. 1984) was the first infrared astronomical satellite which demonstrated the effectiveness of an infrared astronomical mission with a cooled telescope. IRAS carried about 500 L of liquid helium to cool its observation instruments, including a 60 cm telescope. Its mission life was only 10 months due to the short hold time

of liquid helium. ISO, which was a European infrared astronomical satellite with a 60 cm telescope, carried over 2300 L of liquid helium to achieve 2.5-year operation life time in space (Kessler et al. 1996). The first Japanese infrared space mission, IRTS (Murakami et al. 1996), was not a dedicated satellite but was one of the experimental instruments onboard the multi-purpose experiment satellite SFU (Space Flyer Unit). IRTS was launched in 1995 onboard SFU and the mission life of IRTS was about a month, since the amount of liquid helium onboard IRTS was very small (90 L). In summary, previous missions required a huge amount of liquid helium to keep their observation systems cooled for a long time.

The Spitzer Space Telescope (hereafter SPITZER) (Werner et al. 2004), which was launched in 2003, employed a new approach. The telescope was launched at ambient temperature and was cooled on orbit by the combination of radiative cooling and helium boil-off vapor. SPITZER utilized an earth-trailing solar orbit. The major advantage of the orbit is being away from the heat of the earth. Hence the outer shell of the cryostat can be cooled very effectively by radiation and a very long mission life (longer than 5 years) is expected with 337 L of liquid helium (Werner et al. 2004).

Although the SPITZER's approach works very effectively for satellites away from the earth, we cannot apply the same technique directly to satellites in the near-earth orbit, because the heat load from the earth is much higher than that for the SPITZER.

We have developed a different type of cryogenic system; a hybrid cryogenic system, which consists of liquid helium and mechanical cryocoolers. We use this system for AKARI (formerly known as ASTRO-F), which is the first Japanese satellite dedicated for infrared astronomy (Murakami et al. 2007). The orbit of AKARI is a near-earth orbit, and the temperature of the outer shell of the cryostat is much higher than that of SPITZER due to large heat load from the earth. The hybrid-cryogenic design enables us to cool the observation system with modest amount (179 L) of liquid helium for more than a year in the near-earth orbit. The mechanical cryocoolers also enable observations at wavelengths shorter than  $5 \mu\text{m}$  even after the exhaustion of liquid helium.

AKARI carries two focal plane instruments (FPI): Infrared Camera (IRC) (Onaka et al. 2007) and Far-Infrared Surveyor (FIS) (Kawada et al. 2007). The AKARI telescope forms a Ritchey-Chretien system with a primary mirror of 68.5 cm diameter, which is made of a porous silicon carbide (SiC) core and a chemical-vapor-deposited coat of SiC on the surface (Kaneda et al. 2005, Kaneda et al. 2007). All of these instruments must be cryogenically cooled to achieve superior sensitivity.

AKARI was successfully launched from the Uchinoura Space Center, Japan on 2006 February 21 (UT) and was put into a solar synchronous orbit above the twilight zone at the altitude of about 700 km (Murakami et al. 2007).

Hirabayashi et al. (2007) discuss details of the design and pre-flight test of the AKARI cryogenic system. In this paper, we describe the flight operation and the on-orbit performance

**Table 1.** Required cooling capability of the cryogenic system of AKARI.

Parameter	Values
With liquid helium	
IRC body temperature	< 7 K
FIS body temperature	< 3 K
Ge:Ga detector temperature	2.0 - 2.5 K
Stressed Ge:Ga detector temperature	1.7 K
Detector and heater power directly dissipated in the liquid helium	3.4 mW*
Telescope temperature	< 7 K
Hold time of Liq. He	> one year
After the exhaustion of liquid helium	
IRC body temperature	< 35 K
Telescope temperature	< 35 K

\* This is a peak value, and the average heat dissipation is 1.5 mW.

of the AKARI cryogenic system.

## 2. Requirements and Implementation

In this section, we briefly summarize requirements for the AKARI cryogenics and their system implementation.

### 2.1. Requirements

Table 1 summarizes the cooling capability required for the cryogenic system of AKARI. To achieve superior sensitivity, observational instruments must be cooled down to cryogenic temperature. We have two aspects on this issue.

One aspect is to reduce the thermal background from observational instruments lower than natural sky background. The temperature requirement for the AKARI's telescope in table 1 is determined from this point of view. FIS has the most stringent requirement on this issue (Kawada et al. 2007).

The other aspect is to reduce thermal dark current of detectors low enough so that dark current does not limit the sensitivity. The temperature requirements for the two focal plane instruments are determined from this point of view. Since detector arrays on AKARI have different levels of dark current as a function of temperature, each instrument has its own temperature requirement. FIS detectors require the lowest temperature.

The requirement on the hold time of liquid helium is determined to perform the all-sky survey observation in the infrared. Ideally, a half-year period of observation can cover the whole sky. However, due to many practical constraints, such as the moon on the sky and the south

**Table 2.** Specifications of the cryogenic system of AKARI.

Cooling Method		Hybrid system consisting of cryogen and mechanical cryocoolers
Cryogen	Type	Super-fluid liquid helium
	Amount	> 25.0 kg at the launch
	Phase separation	Two sets of porous plugs optimized for different flow rates
Mechanical Cryocoolers	Type	Two-stage Stirling cryocoolers
	Number	Two sets
	Cooling Power	200 mW at 20 K per set
	Nominal Operation	Simultaneous operation of the two sets with half-power operation for each set

Atlantic anomaly near the earth, we cannot cover the whole sky in half a year, and we need at least one year to cover the all sky. Hence the hold time of liquid helium is required to be longer than one year.

One more set of requirements is the temperature of IRC and the telescope after liquid helium runs out. This enables the near-infrared observations with IRC even after helium runs out only with mechanical cryocoolers.

## 2.2. Implementation

Table 2 summarizes specifications of the AKARI cryogenics implemented to meet the requirements in table 1. Figure 1 shows the cross sectional view of the AKARI cryostat and figure 2 illustrates a schematic view of the AKARI cryogenic system.

The AKARI cryogenic system is a hybrid system of cryogen (super-fluid liquid helium) and mechanical cryocoolers (two-stage Stirling cycle coolers). The observational instruments are cooled directly by liquid helium ( $< 2$  K) or by boil-off helium vapor ( $\sim 4 - 10$  K).

Two types of porous plugs (figure 1) are used for phase separation of helium. The two porous plugs are optimized for different flow rates; 5 mg/s for a large porous plug (PP-L) and 0.5 mg/s for a small porous plug (PP-S). The porous plugs are made of sintered alumina, and their size is 20 mm in diameter and 5mm in thickness (Hirabayashi et al. 2007).

The cryocoolers are implemented not to cool observational instruments directly but to reduce the heat leak to the helium tank, and thereby to extend the hold time of cryogen on orbit. Hence the two-stage Stirling coolers are thermally connected to the Inner Vapor Cooled Shields (IVCS), one of the vapor cooled shields which surround the helium tank and the observation system, to reduce the heat load to the helium tank.

In order to reduce the heat load to the helium tank, it is crucial to lower the temperature

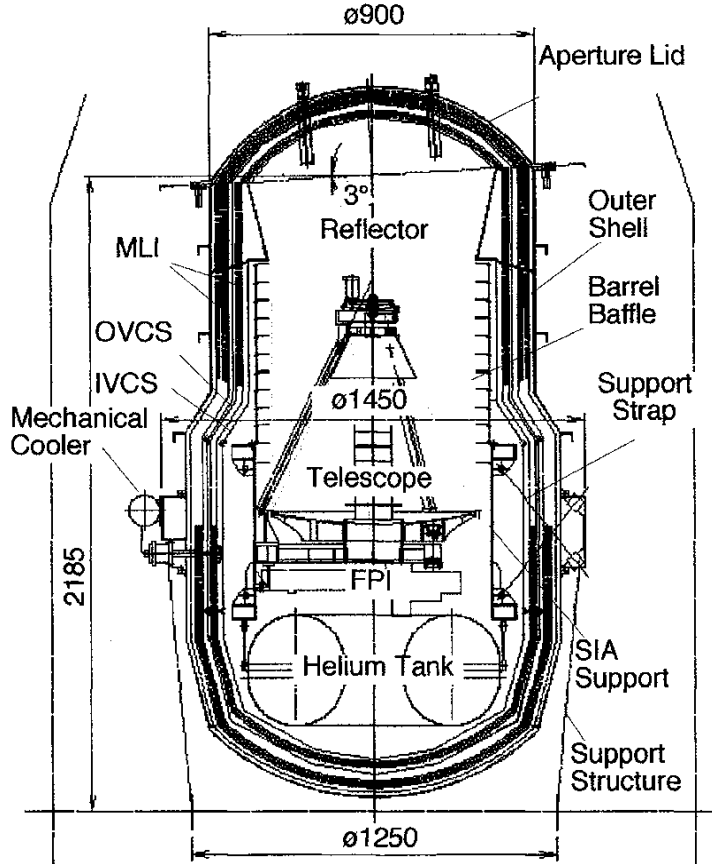


Fig. 1. Cross sectional view of the AKARI cryogenic system.

of the outer shell of the cryostat. To protect the cryostat from the direct radiation from the sun, we put a sun-shield at one side of the cryostat. We also covered the surface of the cryostat with Ag-coated polyetherimide film (Ag/PEI, Ichino et al. 1986) to reduce the absorption in the visible light and to increase the emissivity in the infrared, and thereby to make the radiative cooling effective.

Another key component is the aperture lid (APLD). The aperture lid is designed to keep the vacuum inside the cryostat on the ground and to be jettisoned on orbit after the outgas from the satellite drops significantly and the pressure outside the cryostat approaches to that of the environmental pressure of gas. Since the aperture lid blocks some of the radiation paths from the outer and inner vapor shields, the on-orbit heat load to the helium tank with the aperture lid is estimated to be about three times larger than that after the lid is jettisoned.

### 2.3. Two-stage Stirling cooler

One of the key features of the AKARI cryogenic system is the mechanical cryocoolers. The mechanical coolers adopted for AKARI are two-stage Stirling coolers (Narasaki et al.

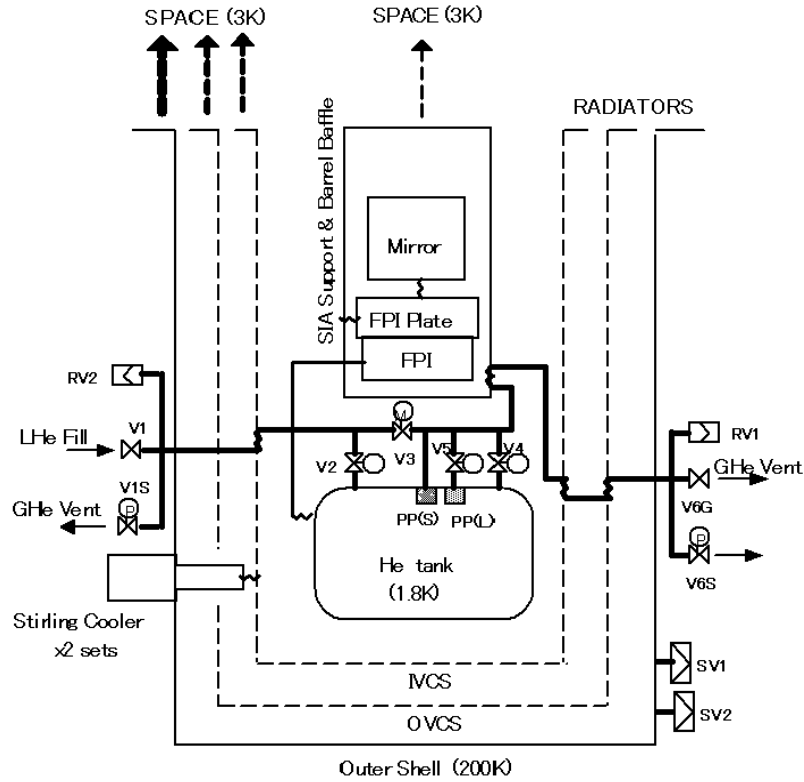


**Fig. 2.** Conceptual view of the AKARI cryogenic system configuration.

2004). Figure 3 shows a cross-sectional view of the two-stage Stirling cooler, which consists of a compressor, two-stage cold head, and a connecting tube. Each set of the cryocoolers weighs about 9.4 kg. Each compressor has two linear pistons operating in opposite directions to reduce its vibration.

The compressors are mechanically and thermally fixed to the outer shell of the cryostat. Hence the heat from the compressors is sunk to the outer shell, which is designed to work also as a radiator for coolers.

On the other hand, the 2nd-stage cold heads of the coolers are thermally connected to the IVCS, and the coolers thereby reduce the heat load to the helium tank as discussed above. Another important role of the cryocoolers is to cool the telescope and IRC to a 30 K-level after liquid helium exhaustion, so that we can continue observations by IRC in the near-infrared.

Two sets of cryocoolers are used for AKARI for redundancy. Each set of the coolers has the cooling capacity of 200 mW at 20 K with the input power of about 100 W. Hence one is enough to meet the cooling requirements. In the nominal operation, however, two sets are operated simultaneously with 50 W input for each set. If one of the cryocoolers fails on orbit,

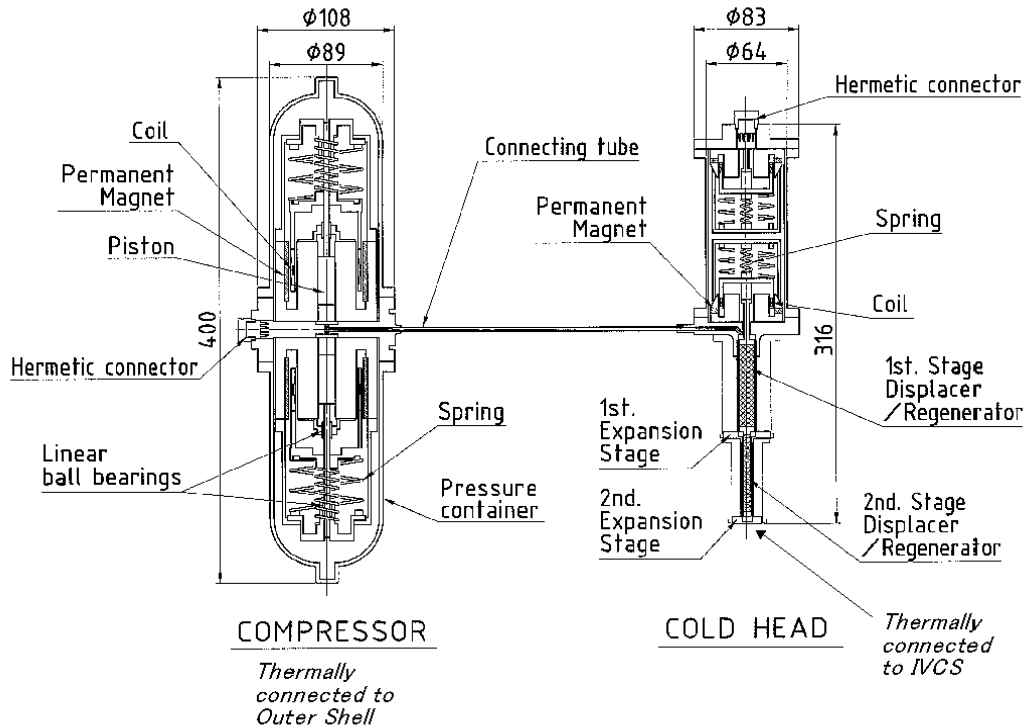


Fig. 3. Cross-sectional view of the two-stage Stirling cryocooler.

we will operate the other cryocooler with the full power (100 W input).

We conducted 40,000 hours of lifetime test for a proto type model of the two-stage Stirling cooler before launch in the laboratory (see also Narasaki et al. 2004). As a result, we did not find any significant degradation in the performance of the cooler.

### 3. Flight operation

In this section, we outline the flight operation of the AKARI cryogenic system. We discuss pre-flight operation, launching operation, and on-orbit operation until the nominal observation phase started.

#### 3.1. Pre-flight operation

The most important task during the pre-flight operation is to fill the helium tank with super-fluid liquid helium (HeII). If the tank is filled with normal liquid helium (HeI) and liquid helium is pumped down to 1.8 K, only 70 % of the whole volume of helium tank ( $V_{\text{Tank}}$ ) can be filled with HeII. Hence transfer of HeII, so-called "top-off", is required just before the launch. A series of final transfer of HeII (top-off) to the helium tank was performed at the launching pad. Figure 4 shows the temperature change during this pre-launch operation phase.

We performed three transfers during the low temperature top-off operation. The third

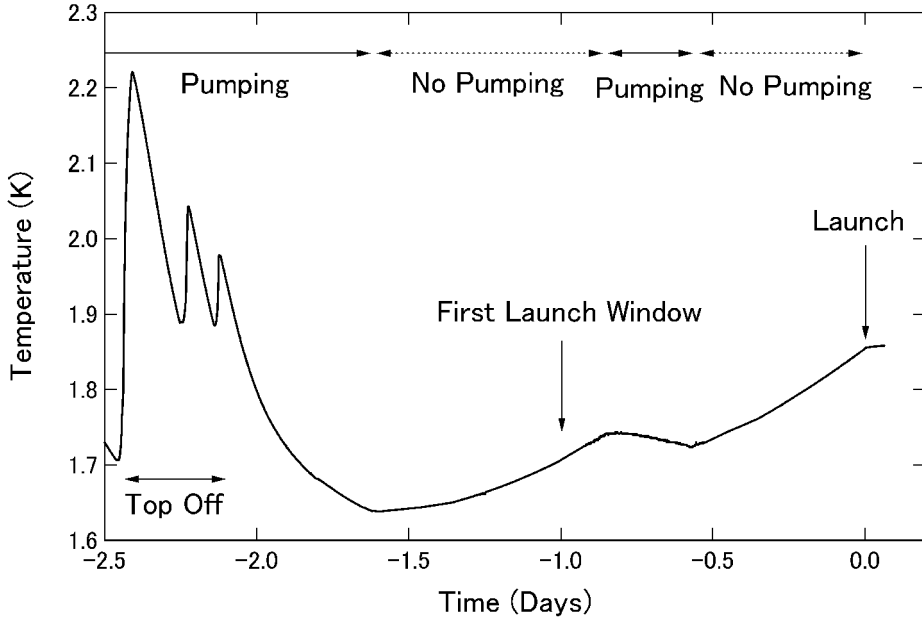


Fig. 4. Temperature change during pre-launch operation.

transfer filled the whole volume (188.7 L) of the helium tank with HeII at the temperature of 1.978 K.

After the third transfer, we pumped down helium for 13.5 hours, and liquid helium cooled from 1.978 K to 1.638 K. We estimated that the tank was filled with 180 L (95.4 % of  $V_{\text{Tank}}$ ) of liquid helium at this point. Then we stopped pumping, closed all valves, and waited for the launch. We tried the first launch on February 20, but the launch was called off because of bad weather.

After the call off, we restarted pumping. Just before we restarted pumping, the temperature of helium was 1.742 K, because the venting valve had been closed for 16 hours. For this 2nd-day operation, we pumped helium about 6 hours, and the temperature of helium went down to 1.725 K. Then we stopped pumping, and closed all the valves. We waited about 14 hours before the launch as shown in figure 4. We estimate that we had 179 L (26.0 kg or 94.9 % of  $V_{\text{Tank}}$ ) of liquid helium at the temperature of 1.854 K (significantly below the  $\lambda$  point of 2.17 K required) at the time of launch. The requirements are the volume of 170 L and the temperature significantly below the  $\lambda$  point of 2.17 K, and they were satisfied at the launch.

### 3.2. Lift off

The AKARI satellite was launched at 21:28 on 2006 February 21 (UT) from the Uchinoura Space Center by a M-V rocket. Table 3 summarizes sequence of events concerning the cryogenics.

**Table 3.** Sequence of events concerning the cryogenic system.

Date (UT)	Time (UT)	Time after launch	Events
Feb.21	21:28:00	0 s	Lift Off
	21:31:50	230 s	He vent valve opened
	21:34:40	400 s	He fill valve opened
Feb.27	11:04:32	5.57 days	Continuous operation of cryocoolers started*
Mar.01	07:08:26	7.40 days	Porous plug L closed
Mar.14	07:35:09	20.42 days	He mass measurement #1
Mar.30	14:34:43	36.71 days	Cryocoolers stopped <sup>†</sup>
Mar.31	08:11:33	37.45 days	Cryocoolers restarted <sup>†</sup>
Apr.13	07:55:11	50.44 days	Aperture lid jettisoned
May 09	21:35:55	77.01 days	He mass measurement #2
Jul.06	21:22:49	135.00 days	He mass measurement #3

\* The cryocoolers had been operated even before this timing but only intermittently.

<sup>†</sup> The cryocoolers stopped during this period due to unexpected behavior of the power line of the satellite.

At the lift-off, all the valves were closed and the cryocoolers were turned off. Temperatures and status concerning the cryogenics were monitored during the launching operation. The upper panel of figure 5 shows the temperature change of the outer shell and the OVCS after the launch. The outer shell started to cool just after the launch, and went below 220 K within half a day after the launch. This quick change of the temperature is attributed to the effective radiative cooling of the outer shell. The lowered temperature of the outer shell reduced the heat load inside the cryostat, and thus the temperature of OVCS decreased gradually after the launch.

The venting valve V6 (figure 2) was opened 230 seconds after the launch, and the boil-off helium gas started to be vented into space. The timing to open the valve V6 was determined, so that the ambient pressure was low enough for boil-off gas to be vented outside the cryostat, while the acceleration that retain the helium toward the bottom of the tank still remained.

The lower panel of figure 5 shows the temperatures of the helium tank ( $T_{\text{He}}$ ) and the down stream of a large porous plug (PP-L) ( $T_{\text{PP-L}}$ ). Before the launch, when the venting valve V6 was closed, the temperature of the down stream of PP-L ( $T_{\text{PP-L}}$ ) was the same with that of the helium tank ( $T_{\text{He}}$ ). On the other hand, immediately after V6 was opened (230s after the launch),  $T_{\text{PP-L}}$  dropped about 0.07 K, which indicated that the porous plug started to work as a phase separator. The small porous plug (PP-S) shows similar behavior.

During a few hours after the launch, the boil-off gas flow rate was so high that the helium

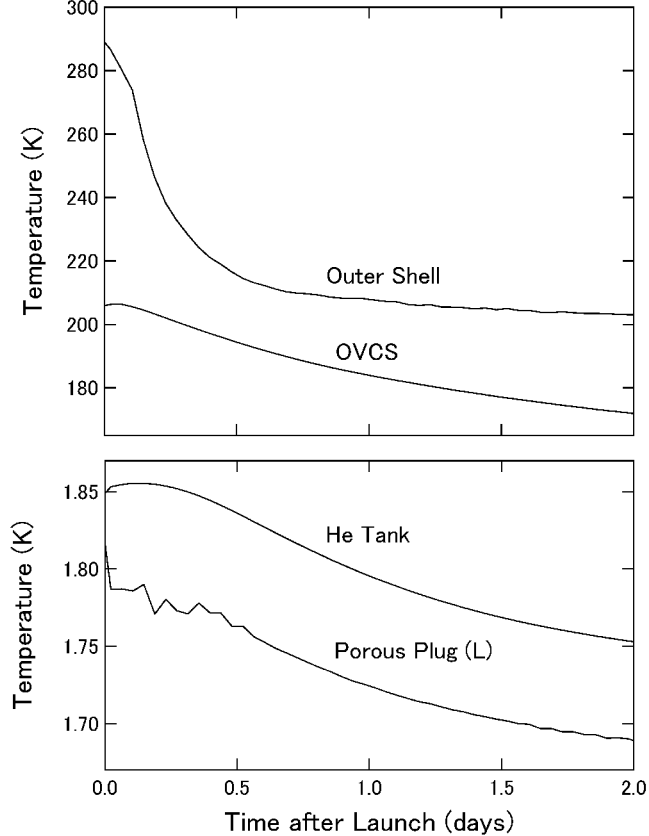


**Fig. 5.** Temperature change after the launch

tank temperature continued to rise for a while. The temperature of the helium tank reached its maximum of 1.86 K about three hours after the launch, and started to go down as OVCS started to be cooled. Oscillation of  $T_{PP-L}$  was observed till about half a day after the launch.

As shown above, the helium tank temperature was always well below the  $\lambda$  point of 2.17 K.

### 3.3. Switching porous plugs

As discussed above, the AKARI cryogenic system has two porous plugs, PP-L and PP-S, which are optimized for flow rates different by an order of magnitude. When the boil-off gas flow rate was still high just after the launch, we used both PP-L and PP-S so that we could keep the helium-tank temperature low enough even with high gas flow rate. But, when the boil-off gas flow rate became low enough that gas venting only through PP-S is enough, we closed the valve V5 to disable PP-L.

Figure 6 shows the temperature change of the helium tank ( $T_{He}$ ) after the launch together with the temperature differences between the downstream of two porous plugs and the helium tank ( $T_{He} - T_{PP-L}$  and  $T_{He} - T_{PP-S}$ ). After the launch, the temperature differences decreased continuously, and the temperature difference between the downstream of PP-S and the helium

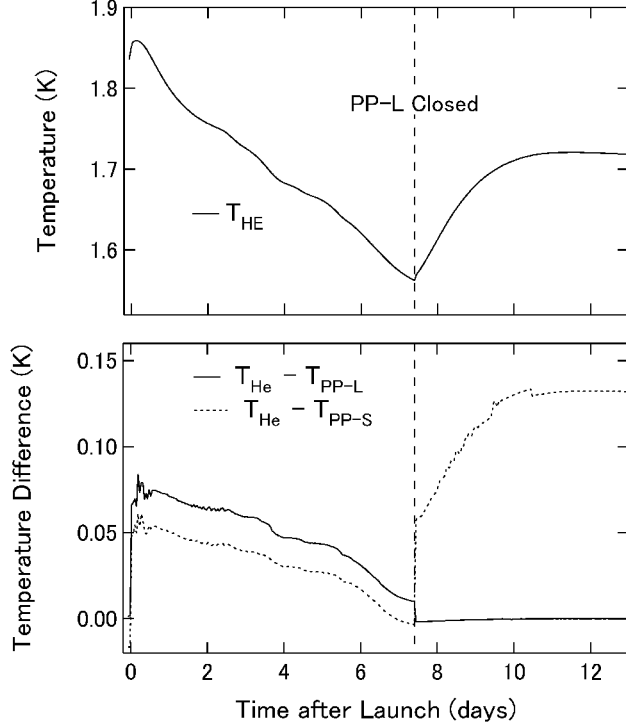


**Fig. 6.** Temperature change concerning the operation of porous-plugs.

tank ( $T_{\text{He}} - T_{\text{PP-S}}$ ) became almost 0 about 7 days after the launch, which indicated that the operation of PP-S could be unstable.

Hence we closed the valve V5 to disable PP-L about 7 days after the launch. Figure 6 also shows the temperature behavior after we closed the V5 valve. After closing the V5 valve, the downstream temperature of PP-L rose to the helium tank temperature, which indicated the termination of the operation of PP-L. On the other hand, the temperature difference between the downstream of PP-S and the helium tank changed from almost 0 K to about 60 mK just after closing V5 valve, which indicated that PP-S became the dominant venting path. Since PP-S has higher impedance than PP-L, the temperature of the liquid helium tank ( $T_{\text{He}}$ ) started to increase gradually after closing the valve. The temperature of the helium tank reached its equilibrium temperature (with aperture lid) of 1.72 K about 3 days after closing the valve. At the same time,  $T_{\text{He}} - T_{\text{PP-S}}$  also increased from 60 mK to 130 mK.

According to the porous-plug component test before the launch, the temperature difference of 130 mK indicates that boil-off rate of helium was 1.67 mg/s. This is consistent with pre-flight tests and prediction of the thermal model of the cryostat.

#### 3.4. *Jettisoning the aperture lid*

Prior to observations, the aperture lid must be jettisoned. The original plan was to keep the aperture lid on the cryostat for 14 days after launch to protect the inside of the cryostat

from contaminants outgassing from the satellite. However, just after launch, we found that on-board solar sensors had problems (Murakami et al. 2007). This forced a delay in the jettison of the aperture lid. We modified the on-board software to cope with solar-sensor problems and then we opened the aperture lid on 2006 April 13, 51 days after launch. As discussed previously, with the aperture lid on, the heat load to the liquid helium is three times larger than that with the aperture lid off. We estimate that the delay in the aperture lid jettison of 37 days results in a loss of 100 days of observation time.

Figure 7 shows the temperature change after jettisoning the aperture lid. All the temperatures concerning the AKARI cryostat started to decrease after the aperture lid was jettisoned. OVCS and IVCS started to be cooled, because they had radiators (figure 2), which had been blocked by the aperture lid and the radiators started to work once the aperture lid was jettisoned. Please note that the IVCS temperature reached its minimum temperature about a week after the aperture lid was jettisoned. This was caused by the balance between the decreasing temperature of OVCS and the boil-off helium gas flow rate, which was still higher than its equilibrium value at this point. After this point, the temperature of IVCS started to rise, since the helium gas flow rate decreased continuously.

As the vapor cooling shields cooled, the helium tank also started to cool gradually. It took about two weeks for the helium tank to reach its equilibrium temperature of 1.5 K.

## 4. Flight performance of the cryogenic system

### 4.1. Comparison with model calculation

The cryogenic system of AKARI reached its equilibrium state about two weeks after jettisoning the aperture lid, and we checked its performance on orbit during the equilibrate phase.

Table 4 shows the comparison of the flight performance of the AKARI cryogenics with the model prediction (Hirabayashi et al. 2007). Since the temperatures of various stages change on orbit due to the change of the heat input from the earth, we take the average values (one week in May 2006) on orbit. As table 4 shows, the flight performance is quite consistent with the model prediction made before launch. One can notice small difference in the temperature of the helium tank (flight value is lower) and in the temperature of the telescope (flight value is higher). This tendency implies that the helium gas flow rate is slightly lower than the model prediction.

### 4.2. Helium mass measurement

We measured the mass of liquid helium by applying the constant heat load (781 mW) to the helium tank for one minute, which makes the total heat of 46.86 J. Figure 8 showed an example of the temperature profile during one of the measurements on orbit. The temperature showed linear increase when the input heater was on, and became quickly stable just after the

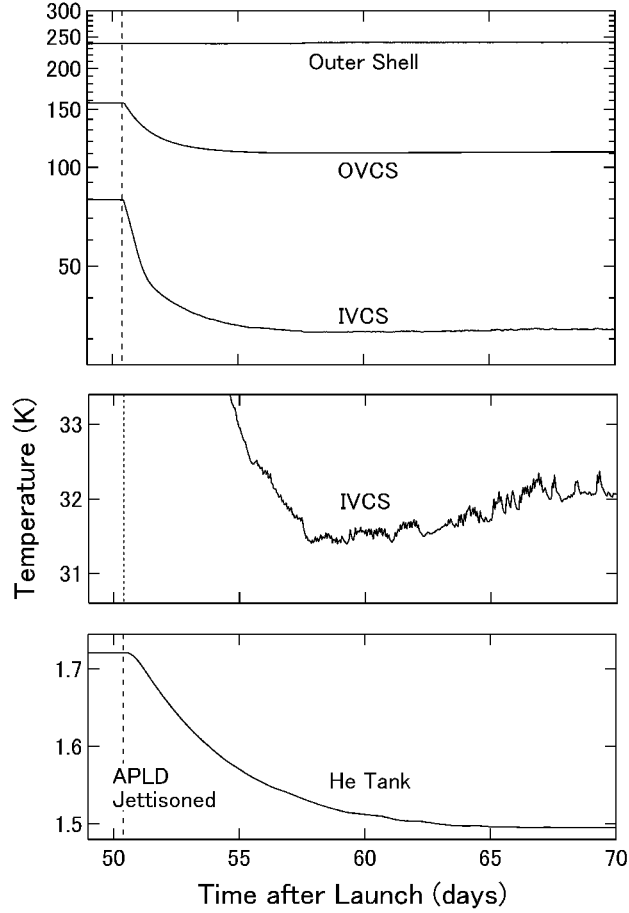
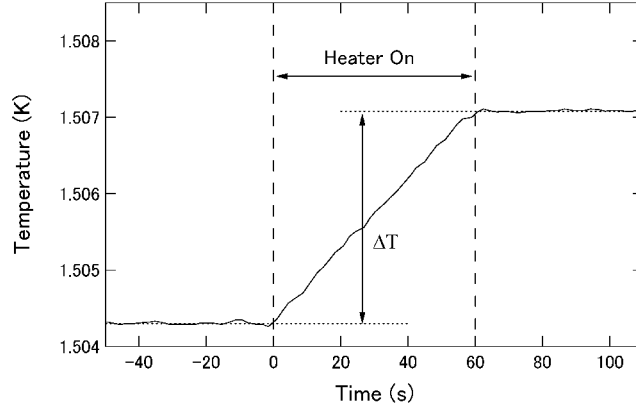


Fig. 7. Temperature change after jettisoning the aperture lid (APLD).

Table 4. Comparison of flight performance with model predictions.

	Measured Values on Orbit			Model
	Max	Min	Average	
He Tank (K)	1.504	1.499	1.502	1.60
Telescope (K)	6.575	5.874	6.175	5.6
Cryocooler (K)	26.10	24.45	24.92	23.9
IVCS(K)	34.31	31.62	32.36	24.6
OVCS(K)	110.8	110.6	110.6	102.0
Outer Shell (K)	244.0	241.9	243.0	238.9
Compressor (K)	248.2	246.3	247.3	240.2
Cryocooler Power (W)	100.2	98.9	99.8	100



**Fig. 8.** Temperature profile during the measurement of liquid helium mass. We turned on a heater for one minute and observed the temperature increase due to the additional heat load.

**Table 5.** Measurements of helium mass.

	Days after launch	$\Delta T$ (mK)	He mass (kg)	comments
#1	20.42	$1.08 \pm 0.03$	$20.95^{+0.21}_{-0.31}$	With aperture lid
#2	77.01	$2.78 \pm 0.03$	$14.71^{+0.15}_{-0.22}$	Without aperture lid
#3	135.00	$3.14 \pm 0.03$	$13.10^{+0.12}_{-0.19}$	Without aperture lid

heater was turned off.

We made the measurement of helium mass three times so far as shown in table 5. The first one was made before the aperture lid was jettisoned and still the boil-off rate of helium gas was higher than the nominal value. The second and the third measurements were performed after the aperture lid was jettisoned and when the helium boil-off rate reached its equilibrium.

From the difference of the second and the third measurements, we estimated that helium gas boil-off rate was  $0.32 \pm 0.07$  mg/s, which is slightly smaller than the model prediction (0.49 mg/s). This tendency is also consistent with the tendency mentioned in the previous subsection on the comparison between the observed temperatures and model predictions.

#### 4.3. Comparison with other satellites

Table 6 shows the comparison of the on-orbit performance of the cryogenic systems of representative infrared astronomical satellites. The second column of table 6 show the boil-off helium gas flow rate ( $\dot{m}$ ) in the equilibrium state on the orbit, the third column shows the heat load to the cryogen ( $P_{\text{He}}$ ) converted from  $\dot{m}$ . AKARI's performance (in terms of the heat load to the cryogen) is much better than those of IRAS, ISO and IRTS and is close to that of SPITZER.

However, each cryostat in Table 6 has a different temperature of the outer shell ( $T_{\text{shell}}$ ),

**Table 6.** Comparison of cryogenic systems for space infrared missions.

	He flow rate	$T_{\text{He}}$	$P_{\text{He}}$	$V_{\text{Tank}}$	$T_{\text{Shell}}$	$H$	$P_{\text{He}}/H$	He hold time	Ref.
	(mg/s)	(K)	(mW)	(L)	(K)	(W)		(days)	
IRAS	2.4	1.80	55.4	545	197	342	$1.6 \times 10^{-4}$	302	(1), (2)
IRTS	4.0	1.91	78.9	100	300	593	$1.3 \times 10^{-4}$	37	(3)
ISO	4.1	1.74	93.6	2342	113	97.9	$9.6 \times 10^{-4}$	873	(2), (4)
SPITZER	0.29	1.24	5.7	360	34	0.230	$2.5 \times 10^{-2}$	1930*	(5), (6)
AKARI	0.32	1.50	7.2	189	243	168	$4.3 \times 10^{-5}$	590*	This work

\* Expected hold time.

Reference: (1) Urbach & Marson (1984), (2) Holmes et al. (2002), (3) Fujii et al. (1996), (4) Seidel (1999), (5) Finley, Hopkins, & Schweickart (2004), and (6) Werner et al. (2004).

and the radiative heat load on cryogen is different. To compare the performance of cryostats with different  $T_{\text{shell}}$ , Holmes et al. (2002) introduces a parameter  $H$ , to which the radiative heat load on the cryogen is proportional.

$$H = \sigma_{\text{B}} A_{\text{Tank}} (T_{\text{shell}}^4 - T_{\text{He}}^4), \quad (1)$$

where  $\sigma_{\text{B}}$  is the Stefan Boltzmann constant and  $A_{\text{Tank}}$  is the surface area of the cryogenic tank. Here we take  $A_{\text{Tank}} = SV_{\text{Tank}}^{2/3}$ , and  $S$  is a geometrical factor for different shape of tanks. We use  $S = 6$  as a representative value for cylindrical tanks (Holmes et al. 2002). The 7th column in table 6 shows the parameter  $H$  and the 8th column shows the parameter ratio  $P_{\text{He}}/H$ , which compares the performance of cryostats with different  $T_{\text{shell}}$ .

The ratio  $P_{\text{He}}/H$  in table 6 shows that IRAS and IRTS have similar performance, which is slightly better than that of ISO, although their sizes are completely different. SPITZER has a very low helium gas flow rate and small  $P_{\text{He}}$ . However, according to the comparisons based on  $P_{\text{He}}/H$ , SPITZER does not show very good performance. The good performance of SPITZER in  $P_{\text{He}}$  is mostly due to its low  $T_{\text{shell}}$ .

On the other hand, AKARI shows the best performance in  $P_{\text{He}}/H$  among the systems listed in table 6. Although AKARI has relatively high outer-shell temperature, its  $P_{\text{He}}$  is close to that of SPITZER, whose  $T_{\text{shell}}$  is much lower than that of AKARI. This is mainly due to the good efficiency of the two-stage Stirling coolers incorporated in the hybrid cryogenic design of AKARI.

The 9th column in table 6 shows the on-orbit hold time of liquid helium. Although the delay in the aperture lid jettison resulted in significant loss of liquid helium, the expected on-orbit hold time of liquid helium for AKARI is longer than 500 days, which meets the requirements discussed in section 2.

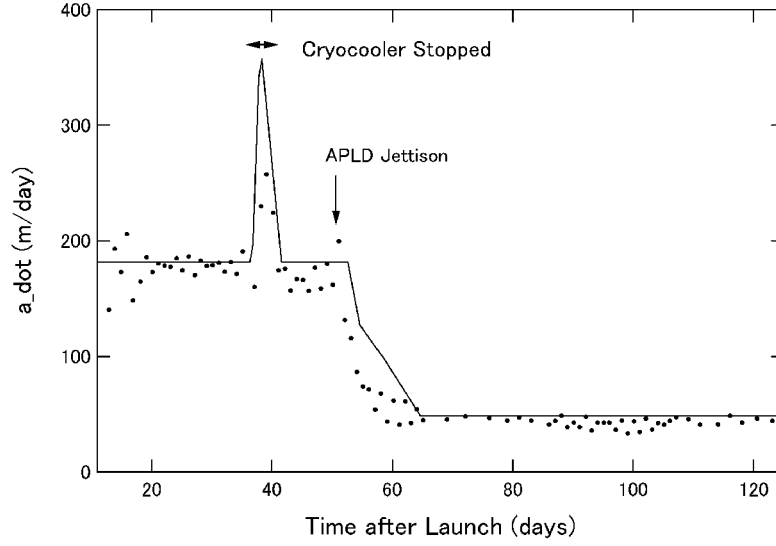


**Fig. 9.** Rate of change of the semi major axis ( $\dot{a}$ ) for the orbit of AKARI. Dots show observed values, while the line indicates values obtained by the equation 4 together with  $\dot{m}$  estimated on the basis of the cryogenic model (Hirabayashi et al. 2007).

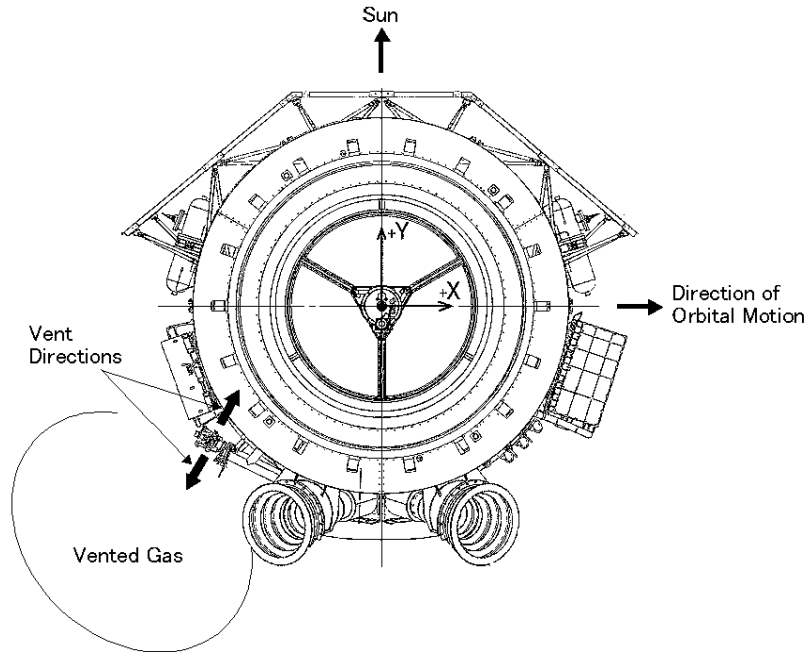


**Fig. 10.** Top view of the AKARI cryostat and the directions of gas vent.

## 5. Orbital change due to vented gas

Soon after the launch, we found that the the AKARI orbit was not descending but ascending day by day. In response to several operations of the cryogenic system, its ascending rate changed quite a lot as shown in figure 9. This implies that the orbital change has something to do with helium gas in the system.

We check the design of the vent path of helium in the AKARI cryogenic system. Vented gas goes to two opposite directions from the venting valves as shown in figure 10, and thereby the total momentum of the flowing helium gas is canceled. However, the pressure due to the thermal motion of the vented gas can push the satellite to one direction, since the gas is predominantly on one side of the satellite as shown in figure 10. The venting valves are located at the angle of 45 degrees from -Y axis to the -X axis as shown in figure 10. Hence the gas can push the satellite both to the +X and +Y directions. Among the two components, +Y vector works to change the inclination of the orbit, but its effect is canceled when averaged in one revolution of the orbit. On the other hand, the other component, +X vector, pushes the satellite toward the direction of the orbital motion of the satellite and hence this can be the  $\Delta V$  component to increase the orbit.

In the following, we make a rough estimate of if this effect can explain the observed orbital change. Small orbital change ( $\Delta r \ll r$ ) due to integrated  $\Delta v$  can be written as follows (Wertz & Larson 1999):

$$\Delta v = \frac{\Delta r}{2r} \sqrt{\frac{GM_E}{r}}, \quad (2)$$

where  $r$  is the radius of the orbit (here we assume a circular orbit for simplicity) and  $M_E$  is the mass of the earth.

If we assume that the gas is in thermal equilibrium, we can write the average gas thermal velocity  $v_{\text{th}}$  as a function of temperature as follows:

$$\frac{3}{2}kT = \frac{1}{2}mv_{\text{th}}^2. \quad (3)$$

Here we assume that the gas motion is completely isotropic, and only one third of the total energy will contribute to pushing the satellite, then the conservation of the momentum gives us the following,

$$M_{\text{sat}} \Delta v_{\text{day}} = \frac{2}{\sqrt{2}\sqrt{3}} \dot{m} t_{\text{day}} v_{\text{th}} \eta, \quad (4)$$

where  $M_{\text{sat}}$  is the mass of satellite,  $\Delta v_{\text{day}}$  is  $\Delta v$  integrated in one day,  $\dot{m}$  is helium gas flow rate,  $t_{\text{day}}$  is the length of one day, and  $\eta$  is the efficiency of this effect.

We use  $T = 240$  K (outer shell temperature) and  $r = 700$  km, and we get the following relation between  $\dot{r}$  and  $\dot{m}$ :

$$\dot{r} = 49 \left( \frac{\eta}{0.8} \right) \left( \frac{\dot{m}}{0.32 \text{ mg/s}} \right) \text{ m/day}. \quad (5)$$

This  $\dot{r}$  (circular orbit) can be compared with the observed  $\dot{a}$  (elliptical orbit), since AKARI's orbit is very close to circular. Figure 9 also shows a theoretical curve which is derived by using  $\dot{m}$  estimated from the cryogenic model with  $\eta = 0.8$ .

The observed orbital change can be reasonably explained by the model prediction. Hence we conclude that the orbital change is due to the effect that thermal pressure of the vented gas is pushing the satellite.

## 6. Summary

The thermal behavior of the AKARI cryogenic system has been presented. The AKARI cryogenic system employs a hybrid system, consisting of cryogen (liquid helium) and mechanical coolers (2-stage Stirling coolers). With the help of the mechanical coolers, 179 L of liquid helium can keep the instruments cryogenically cooled for more than 500 days. The on-orbit performance of the AKARI cryogenics is consistent with the design and pre-flight test, and is much better than those of previous missions. Although the cryostat vent was designed to prevent thrust from the venting helium gas, a very small thrust from the venting helium is observed anyway. This effect is reasonably explained by the thermal pressure of the helium gas exerted at the vent site which is on the only one side of the space craft.

## Acknowledgements

AKARI is a JAXA project with the participation of ESA. We are deeply grateful to all the members of the AKARI team for their continuous support. We would like to cordially thank the M-V rocket team for their help during the launching operation. This work was supported in part by a Grant-in-Aid for Scientific Research from Japan Society for the Promotion of Science (No. 15204013).

## References

- Finley, P.T., Hopkins, R.A., & Schweickart, R.B. 2004, Proc. SPIE, 5487, 26
- Fujii, G., Tomoya, S., Kyoya, M., Hirabayashi, M., Murakami, M., Matsumoto, T., Hirao, T., Murakami, H., Okuda, H., & Kanari, T. 1996, Cryogenics, 36, 731
- Hirabayashi, M, Narasaki, K., Tsunematsu, S., Kimura, Y., Yoshida, S., Murakami, H., Nakagawa, T., Ohnishi, A., Matsumoto, T., Kaneda, H., Enya, K., & Murakami, M. 2007, Cryogenics, submitted
- Holmes, W, Cho, H., Hahn, I., Larson, M., Schweickart, R., & Volz, S. 2002, Cryogenics, 41, 865
- Ichino, T., Sasaki, S., & Hasuda, Y. 1986, Transactions of Institute Electronics & Communication Engineers of Japan, J69-C, 199 (in Japanese)
- Kaneda, H., et al. 2005, Appl. Opt., 44, 6823
- Kaneda, H., et al. 2007, PASJ, in this volume
- Kawada, M., et al. 2007, PASJ, in this volume

Kessler, M. F., et al. 1996, A&A, 315, L27  
Murakami, H., et al. 1996, PASJ, 48, L41  
Murakami, H., et al. 2007, PASJ, in this volume  
NarasakiAK., et al. 2004, Advances in Cryogenic Engineering, 49B, 1428  
Neugebauer, G., et al. 1984, ApJ, 278, L1  
Onaka, T., et al. 2007, PASJ, in this volume  
Seidel, A. 1999, Cryogenics, 39, 135  
Urbach, A.R. & Mason, P.V. 1984, Advances in Cryogenic Engineering, 29, 651  
Werner, M. W., et al. 2004, ApJS, 154, 1  
Wertz, J. R. & Larson, W. J.1999, Space Mission Analysis and Design (Reidel: Kluwer Academic Publishers) 148